Visible-light sensitisation of near-infrared luminescence from Yb(III), Nd(III) and Er(III) complexes of 3,6-bis(2-pyridyl)tetrazine

Nail M. Shavaleev,[a] Simon J. A. Pope,[b] Zöe R. Bell,[a] Stephen Faulkner *[b] and Michael D. Ward *[a]

[a] School of Chemistry, University of Bristol, Cantock's Close, Bristol, UK BS8 1TS.
    E-mail: mike.ward@bristol.ac.uk
[b] Department of Chemistry, University of Manchester, Oxford Road, Manchester,
    UK M13 9PL. E-mail: stephen.faulkner@man.ac.uk

Reaction of the potentially bis-bidentate bridging ligand 3,6-bis(2-pyridyl)tetrazine (BPTZ) with various lanthanide complexes [Ln(tta)$_3$(H$_2$O)$_2$] [Htta = thenoyl(trifluoro)acetone; Ln = La, Nd, Gd, Er, Yb] in aqueous ethanol afforded the mononuclear complexes [Ln(tta)$_3$(BPTZ)] (Ln = La, Nd) or the dinuclear complexes [{Ln(tta)$_3$}$_2$(μ-BPTZ)] (Ln = Gd, Er, Yb) in which one or two, respectively, lanthanide tris-diketonate {Ln(tta)$_3$} units are bound to the N,N-bidentate compartments of BPTZ. Crystal structures of the dinuclear complexes [{Yb(tta)$_3$}$_2$(μ-BPTZ)]·CH$_2$Cl$_2$ and [{Gd(tta)$_3$}$_2$(μ-BPTZ)]·2CH$_2$Cl$_2$ show that the metal centres have an approximately square-antiprismatic eight-coordinate geometry; there are close contacts above and below the plane of the BPTZ bridging ligand between peripheral trifluoromethyl groups from a tta ligand associated with each metal centre. It is not apparent why the larger lanthanides La and Nd only give a mononuclear complex whereas the smaller lanthanides Gd, Er and Yb give the dinuclear complex in each case. UV/Vis spectroscopic titrations of a solution of BPTZ in CH$_2$Cl$_2$ with increasing amounts of [Ln(tta)$_3$(H$_2$O)$_2$] (Ln = La and Yb) show very similar behaviour, with stepwise binding constants K_1 and K_2 for association of the two {Ln(tta)$_3$} units of ca. 10^6 M^{-1} and 10^5 M^{-1}; allowing for the expected statistical factor of 4 there is an additional reduction in the value of K_2 compared to K_1 which may be associated with a steric interaction between the two {Ln(tta)$_3$} units when the dinuclear complex forms. Steady-state and time-resolved luminescence studies on the complexes with Yb, Nd and Er, both in the solid state and CH$_2$Cl$_2$ solution, show that near-IR luminescence on the microsecond timescale can be sensitised by irradiation either at 337 nm into the tta-based transition, or at 520 nm into the low-energy BPTZ-centred transition.

Introduction

Luminescent lanthanide complexes have a variety of characteristics which make them of particular value in sensors and display devices, and indeed complexes of Tb(III) and Eu(III)—which emit strongly in the visible region of the spectrum—are employed for applications such as fluoroimmunoassay and fluorescence microscopy where the long luminescence lifetime and sharp, line-like emission make detection particularly easy.[1] Recently there has developed interest in the photophysical properties of lanthanide complexes which are luminescent in the near-IR region, such as Yb(III), Nd(III), Pr(III) and Er(III); compared to Eu(III) and Tb(III) there are relatively few studies on such complexes.[2–7] There are two particular driving forces for this recent interest in near-IR luminescence. Firstly, for *in vivo* imaging it is necessary that the emitted light is at a wavelength where biological tissue is transparent; and whilst human tissue, for example, is opaque to UV and most visible light it is more transparent to red and near-IR radiation. Secondly, near-IR emitting lanthanides are used for optical amplification in lasers [*e.g.* Nd(III), the basis of the common 1064 nm laser][8] and in silica-based fibre optic networks, where the emission wavelengths of Pr(III) (*ca.* 1330 nm) and Er(III) (*ca.* 1550 nm) closely match the 'windows of transparency' in silica used for telecommunications.[9]

There are three important principles to take into account when designing complexes optimised for near-IR emission. Firstly, effective sensitisation of near-IR emission requires energy-transfer from a strongly absorbing antenna group—usually an organic chromophore—to overcome the difficulty of direct excitation into the parity-forbidden, and hence extremely weak, f–f transitions.[10] For energy transfer from the sensitiser to work requires that its lowest energy triplet state lies above (by 1000–2000 cm^{-1}) the energy of the emitting state of the

lanthanide.[11] With near-IR emitters this allows use of relatively long wavelength light for excitation which has important practical advantages. For medical imaging, for example, it means that excitation of the probe (as well as the resultant emission) can occur at a long wavelength to which tissue is relatively transparent. For optical devices, long wavelength sensitisation will allow use of the cheap and widely available semiconductor diode lasers in the red region of the spectrum. To this end sensitisation of near-IR lanthanide emission has been demonstrated using chromophores such as fluoroscein, eosin and fluorexon which have absorption maxima at *ca.* 500 nm.[5] Secondly, the antenna group must be close to the metal to overcome the strong distance-dependence of the energy-transfer process and minimise competing deactivation of its triplet state by oxygen. Finally, the low-energy excited states responsible for near-IR emission are easily quenched by nearby O–H, N–H and C–H oscillators.[2–7] It is therefore desirable to minimise the number of these close to the metal centre by using *e.g.* C–D or C–F bonds instead of C–H.[3,6i]

We describe here the syntheses and photophysical properties of a series of near-IR emitting lanthanide complexes embodying all of these principles to some extent; the complexes are listed in Scheme 1. The synthesis of these complexes is based on the well-known formation of eight-coordinate adducts between {Ln(dik)$_3$} units (Ln denotes a generic lanthanide; dik = a β-diketonate) and N,N-bidentate chelates such as 2,2′-bipyridine (bpy) or 1,10-phenanthroline (phen);[12] we have exploited this recently in the formation of heterodinuclear d–f complexes with various bis-diimine bridging ligands.[13] In the new complexes described in this paper (Scheme 1), the diimine ligand is 3,6-bis(2-pyridyl)tetrazine (BPTZ)[14] which plays two roles. Firstly it acts in the familiar manner as a ligand coordinating to the lanthanide centres using its N,N-bidentate chelating sites. In addition, and in contrast to ligands such as bpy and
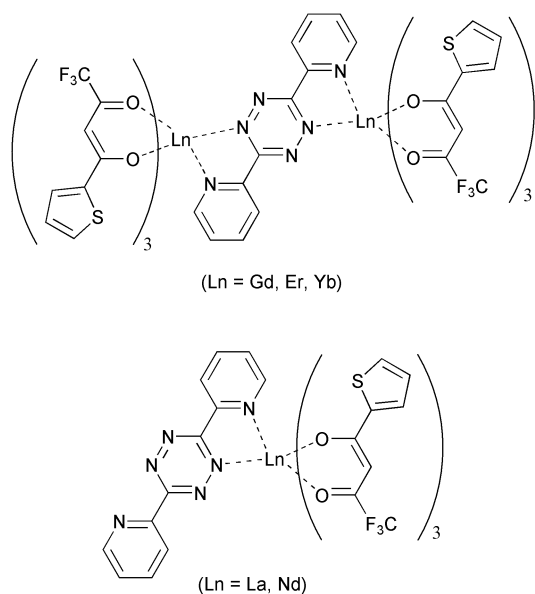
Scheme 1 New complexes described in this paper.

phen, the tetrazine unit provides a moderately intense low-energy chromophore (absorption maximum, about 550 nm; ε ca. 500 M^{-1} cm^{-1}) for long wavelength excitation; this chromophoric unit is directly coordinated to the metal for optimal sensitisation of the metal luminescence. The terminal diketonate ligands are [tta]$^-$ [where Htta = thenoyl(trifluoro)acetone], in which there is only one C–H oscillator close to the metal centre.

Results and discussion

Syntheses and structures of complexes

The new complexes were prepared by reaction of BPTZ with two equivalents of the appropriate [Ln(tta)$_3$(H$_2$O)$_2$] [prepared *in situ* from the hydrated lanthanide(III) chloride, three equivalents of Htta, and NaOH]. In every case the stoichiometry used was based on the assumption that dinuclear complexes [{Ln(tta)$_3$}$_2$(μ-BPTZ)] would form with one metal fragment in each *N,N*-bidentate binding site of BPTZ. For the smaller lanthanides Er and Yb this assumption was correct with good yields of the dinuclear complexes being obtained; the crystal structure of [{Yb(tta)$_3$}$_2$(μ-BPTZ)]·CH$_2$Cl$_2$ is shown in Fig. 1 with selected bond lengths and angles in Table 1. The complex lies on a crystallographic inversion centre (at the centre of the tetrazine ring). In the BPTZ bridging ligand the two pyridyl rings are mutually *transoid*, and the Yb ⋯ Yb separation is 7.817(5) Å. The metal centres have the usual eight-coordinate
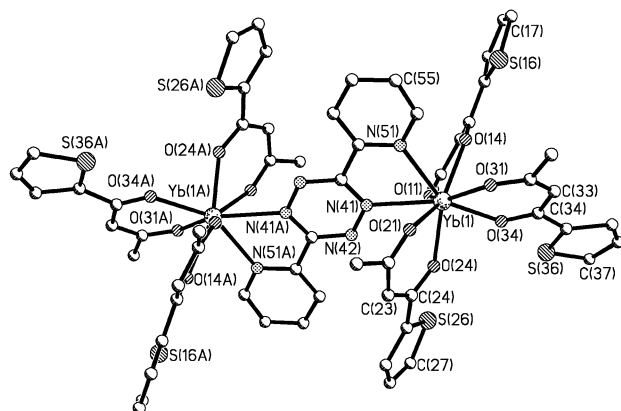
Fig. 1 Molecular structure of [{Yb(tta)$_3$}$_2$(μ-BPTZ)]·CH$_2$Cl$_2$; F atoms on the tta ligands are omitted for clarity.

Table 1 Selected bond lengths (Å) and angles (°) for the two crystal structures

[{Gd(tta)$_3$}$_2$(μ-BPTZ)]·2CH$_2$Cl$_2$		[{Yb(tta)$_3$}$_2$(μ-BPTZ)]·CH$_2$Cl$_2$	
Gd(1)–O(14)	2.314(4)	Yb(1)–O(24)	2.239(9)
Gd(1)–O(21)	2.317(4)	Yb(1)–O(11)	2.247(11)
Gd(1)–O(31)	2.322(4)	Yb(1)–O(34)	2.257(10)
Gd(1)–O(34)	2.325(4)	Yb(1)–O(31)	2.259(10)
Gd(1)–O(24)	2.369(4)	Yb(1)–O(14)	2.286(8)
Gd(1)–O(11)	2.372(4)	Yb(1)–O(21)	2.305(10)
Gd(1)–N(51)	2.595(5)	Yb(1)–N(41)	2.555(10)
Gd(1)–N(41)	2.636(4)	Yb(1)–N(51)	2.520(11)
O(14)–Gd(1)–O(21)	82.43(14)	O(24)–Yb(1)–O(11)	81.5(4)
O(14)–Gd(1)–O(31)	118.18(13)	O(24)–Yb(1)–O(34)	74.9(3)
O(21)–Gd(1)–O(31)	142.21(13)	O(11)–Yb(1)–O(34)	79.5(4)
O(14)–Gd(1)–O(34)	77.03(13)	O(24)–Yb(1)–O(31)	116.4(3)
O(21)–Gd(1)–O(34)	81.72(14)	O(11)–Yb(1)–O(31)	143.3(3)
O(31)–Gd(1)–O(34)	73.68(13)	O(34)–Yb(1)–O(31)	75.5(4)
O(14)–Gd(1)–O(24)	149.68(14)	O(24)–Yb(1)–O(14)	149.6(4)
O(21)–Gd(1)–O(24)	72.38(13)	O(11)–Yb(1)–O(14)	74.3(4)
O(31)–Gd(1)–O(24)	76.37(13)	O(34)–Yb(1)–O(14)	82.6(3)
O(34)–Gd(1)–O(24)	82.78(14)	O(31)–Yb(1)–O(14)	76.2(3)
O(14)–Gd(1)–O(11)	72.51(13)	O(24)–Yb(1)–O(21)	73.8(3)
O(21)–Gd(1)–O(11)	135.67(13)	O(11)–Yb(1)–O(21)	136.5(3)
O(31)–Gd(1)–O(11)	82.10(13)	O(34)–Yb(1)–O(21)	125.6(3)
O(34)–Gd(1)–O(11)	125.17(14)	O(31)–Yb(1)–O(21)	80.1(3)
O(24)–Gd(1)–O(11)	137.74(13)	O(14)–Yb(1)–O(21)	136.6(3)
O(14)–Gd(1)–N(51)	133.98(13)	O(24)–Yb(1)–N(51)	135.6(3)
O(21)–Gd(1)–N(51)	104.63(14)	O(11)–Yb(1)–N(51)	106.0(4)
O(31)–Gd(1)–N(51)	83.95(14)	O(34)–Yb(1)–N(51)	149.1(3)
O(34)–Gd(1)–N(51)	148.53(14)	O(31)–Yb(1)–N(51)	83.7(4)
O(24)–Gd(1)–N(51)	70.44(14)	O(14)–Yb(1)–N(51)	70.3(4)
O(11)–Gd(1)–N(51)	71.49(13)	O(21)–Yb(1)–N(51)	71.4(3)
O(14)–Gd(1)–N(41)	78.23(13)	O(24)–Yb(1)–N(41)	78.2(3)
O(21)–Gd(1)–N(41)	71.80(14)	O(11)–Yb(1)–N(41)	71.6(4)
O(31)–Gd(1)–N(41)	139.81(14)	O(34)–Yb(1)–N(41)	142.9(4)
O(34)–Gd(1)–N(41)	145.73(14)	O(31)–Yb(1)–N(41)	140.5(3)
O(24)–Gd(1)–N(41)	108.49(13)	O(14)–Yb(1)–N(41)	110.4(3)
O(11)–Gd(1)–N(41)	67.71(13)	O(21)–Yb(1)–N(41)	68.7(3)
N(51)–Gd(1)–N(41)	62.13(13)	N(51)–Yb(1)–N(41)	64.0(3)

square antiprismatic coordination geometry, with O(21), O(24), O(31) and O(34) constituting one (approximate) square plane, and N(41), N(51), O(11) and O(14) the other. The metal–ligand distances and angles are unremarkable. Of particular significance from the point of view of luminescence properties is the distance from the metal centres to adjacent C–H oscillators. Non-bonded Yb ⋯ H separations of ≥6 Å can be ignored as those C–H units will not cause significant quenching.[3] Within this distance lie the protons attached to the C^6 and C^5 positions of the pyridyl ring (3.35 and 5.40 Å respectively from the Yb atom), and the three protons at the central positions of the [tta]$^-$ ligands (all between 4.6 and 4.7 Å from the Yb atom). It is noteworthy that there are close non-bonded F ⋯ F contacts between the trifluoromethyl groups of ligands attached to the different metal centres. The F(221) ⋯ F(12C) contact, and its symmetry equivalent F(123) ⋯ F(22A), which lie 'above' and 'below' the BPTZ ring, have an F ⋯ F separation of 2.92 Å, only slightly greater than the sum of the van der Waals radii for the two atoms (2.70 Å).

We also prepared and structurally characterised the analogous dinuclear Gd(III) complex [{Gd(tta)$_3$}$_2$(μ-BPTZ)]. The crystal structure of [{Gd(tta)$_3$}$_2$(μ-BPTZ)] (Fig. 2, Table 1) was also determined and is very similar to that of [{Yb(tta)$_3$}$_2$(μ-BPTZ)], with crystallographically imposed inversion symmetry. The differences in metal–ligand bond lengths are as would be expected based on the ionic radii of the two metals. The Gd(III) centres are again approximately square antiprismatic, with N(41), N(51), O(21), O(24) defining one square plane and O(11), O(14), O(31), O(34) the other; the Gd ⋯ Gd separation is 7.9360(17) Å, and the closest F ⋯ F contact between the trifluoromethyl groups associated with each metal is 2.98 Å (this close contact is emphasised in the view in Fig. 2).
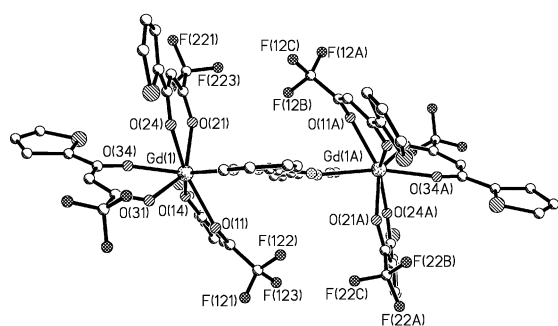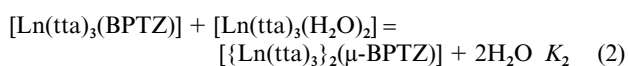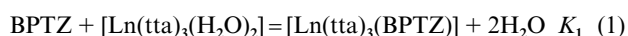
Fig. 2 Molecular structure of [{Gd(tta)$_3$}$_2$(μ-BPTZ)]·2CH$_2$Cl$_2$, emphasising the close proximity of the trifluoromethyl groups above and below the plane of the bridging ligand.

With the larger metal ions La(III) and Nd(III) however the mononuclear complex [Ln(tta)$_3$(BPTZ)] was the only product, even in the presence of excess [Ln(tta)$_3$(H$_2$O)$_2$]. This was shown clearly by the elemental analyses, electronic spectra (see below), and the proton NMR spectrum of the diamagnetic La(III) complex in CD$_2$Cl$_2$, in which the ratio of the tta protons to the BPTZ protons was 3 : 2 (*i.e.* 12 : 8, as required for the mononuclear complex). Interestingly the two pyridyl rings of the BPTZ ligand did not give inequivalent signals: we might expect eight resonances of relative intensity 1H each, four each from the free and coordinated pyridyl rings. Instead, we observed four signals for the BPTZ protons of intensity 2H each, indicating that rapid exchange of the {La(tta)$_3$} unit between the two sites renders them equivalent on the NMR timescale. The presence of only one {La(tta)$_3$} unit *per* BPTZ ligand is however quite clear from the relative intensities of the tta and BPTZ signals, and this confirms the mononuclear nature of [Ln(tta)$_3$(BPTZ)].

The reason for this may be steric, with La(III) and Nd(III) being larger than Gd(III), Yb(III) and Er(III), and may arise from the close contact described above between peripheral F atoms associated with the separate metal centres in the dinuclear complexes. It is possible, for example, that the greater ionic radius of *e.g.* Nd(III) compared to Yb(III) and Er(III) ($\Delta > 0.1$ Å) would result in greater spatial extension of the ligands and, possibly, a more strongly unfavourable steric interaction between the adjacent trifluoromethyl groups of the two components, which will destabilise the dinuclear complex. Electronic effects in contrast do not appear to be significant. It is to be expected that binding of the first Ln(III) unit to the BPTZ ligand would diminish the ability of BPTZ to bind a second, as the Lewis-acidic lanthanide fragment would tend to withdraw electron density from the tetrazine unit and make it less basic. If this were significant however we would see the opposite effect, with the smaller (more Lewis-acidic) lanthanides giving mononuclear complexes.

Equilibrium constants in solution

We measured the formation constants of representative BPTZ complexes in solution to try and shed some light on why the larger lanthanides give only mononuclear complexes. Association of {Ln(dik)$_3$} fragments to simple diimine ligands is reversible,[12] with association constants of the order of 10^7 M^{-1} in CH$_2$Cl$_2$. For formation of the dinuclear complexes with BPTZ there will be two stepwise association constants [eqns. (1) and (2)].

$$\text{BPTZ} + [\text{Ln(tta)}_3(\text{H}_2\text{O})_2] = [\text{Ln(tta)}_3(\text{BPTZ})] + 2\text{H}_2\text{O} \quad K_1 \quad (1)$$

$$[\text{Ln(tta)}_3(\text{BPTZ})] + [\text{Ln(tta)}_3(\text{H}_2\text{O})_2] =$$
$$[\{\text{Ln(tta)}_3\}_2(\mu\text{-BPTZ})] + 2\text{H}_2\text{O} \quad K_2 \quad (2)$$

Addition of increasing amounts of [Yb(tta)$_3$(H$_2$O)$_2$] in CH$_2$Cl$_2$ to a solution of BPTZ in CH$_2$Cl$_2$ caused the absorb-

ance in the 400–500 nm region, arising from the BPTZ-centred transition, to increase markedly as the {Yb(tta)$_3$} fragments bind (see below for a full discussion of the electronic spectra). A plot of absorbance at 460 nm *vs.* number of equivalents of added [Yb(tta)$_3$(H$_2$O)$_2$] is shown in Fig. 3(a), and the curve fits very well to a 1 : 2 host : guest binding model in agreement with eqns. (1) and (2), with $K_1 = 1.0 \times 10^6$ M^{-1} and $K_2 = 7.5 \times 10^4$ M^{-1}. If the binding sites are equivalent and independent we expect $K_1 = 4K_2$ for statistical reasons, because the first binding event can occur at one of two sites whereas only one site is available for the second binding event.† We see here that K_1 is greater than K_2 by a factor of *ca.* 13; even allowing for the statistical effect, it is apparent that that binding of the first {Yb(tta)$_3$} fragment inhibits binding of the second, reducing K_2 by a factor of more than 3, possibly due to the steric interaction identified in the crystal structures of the dinuclear complexes.
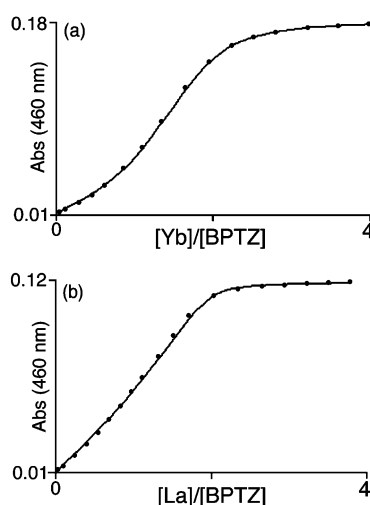

Fig. 3 Results of UV/Vis spectroscopic titrations of BPTZ (1.59 × 10^{-4} M solution in CH$_2$Cl$_2$) with portions of (a) [Yb(tta)$_3$(H$_2$O)$_2$] and (b) [La(tta)$_3$(H$_2$O)$_2$]. Measured data points are black circles; the line through them is the calculated best fit used to derive the stability constant values given in the main text.

An identical experiment using BPTZ and [La(tta)$_3$(H$_2$O)$_2$] gave the similar titration curve in Fig. 3(b), which again fits well to a 1 : 2 host : guest binding isotherm with association constants $K_1 = 2.1 \times 10^6$ M^{-1} and $K_2 = 2.8 \times 10^5$ M^{-1}. Allowing for the statistical factor of 4† we see that binding of the first {La(tta)$_3$} fragment causes only a modest inhibition of binding of the second {La(tta)$_3$} fragment, with K_2 being reduced only by a factor of *ca.* 2 such that formation of the dinuclear complex can occur readily. In fact there is a higher overall formation constant under these conditions for the dinuclear La complex ($\beta = K_1K_2$), which could not be isolated using our synthetic procedure, than for the dinuclear Yb complex which was isolated with no trouble. Given that there is clearly no thermodynamic problem with formation of dinuclear complexes of the larger lanthanides in CH$_2$Cl$_2$, isolation of mononuclear [Ln-(tta)$_3$(BPTZ)] (Ln = La, Nd) must be related to the fact that the syntheses (precipitation of the complexes from aqueous ethanol by addition of water) are not carried out under the same conditions as the titration (solutions allowed to reach equilibrium in CH$_2$Cl$_2$). Whatever the reason it is clear from

---

† Alternatively, one can quote the *microscopic* association constants K^{mic} in which this statistical factor is removed, such that $K_1^{\text{mic}} = 0.5K_1$ and $K_2^{\text{mic}} = 2K_2$. In this case, equivalent and independent binding sites would give $K_1^{\text{mic}} = K_2^{\text{mic}}$ and any deviation from this directly reflects the interaction between the two sites. For [{Yb(tta)$_3$}$_2$(μ-BPTZ)] we have $K_1^{\text{mic}} = 5 \times 10^5$ M^{-1} and $K_2^{\text{mic}} = 1.5 \times 10^5$ M^{-1}; for [{La(tta)$_3$}$_2$(μ-BPTZ)] we have $K_1^{\text{mic}} = 1.1 \times 10^6$ M^{-1} and $K_2^{\text{mic}} = 5.6 \times 10^5$ M^{-1}. The reduced binding affinity of the second metal fragment is then immediately obvious from comparison of K_1^{mic} and K_2^{mic}.

these results that any steric or electronic interactions by which binding of the first {La(tta)₃} fragment inhibits binding of the second, although they are clearly present, are rather modest.

Electronic spectra of the complexes

The electronic spectra of representative complexes are shown in Fig. 4. Two points are immediately clear. Firstly, the region of the spectrum where the absorbance characteristic of the {Ln(tta)}₃ units occurs (330–400 nm) confirms the nuclearity of the complexes. Thus, the absorbance of mononuclear [Nd(tta)₃(BPTZ)] in this region is about the same as that of [Nd(tta)₃(H₂O)₂], but half that of dinuclear [{Yb(tta)₃}₂-(μ-BPTZ)]. In other words, the spectral features associated with the {Ln(tta)}₃ units are additive. Secondly, the low-energy transition of BPTZ which is responsible for its red colour occurs in the complexes at a wavelength (500–550 nm) where there is no competing absorption from the {Ln(tta)₃} units, *i.e.* completely selective excitation of the bridging ligand chromophore is possible. An important advantage of this is that free [Ln(tta)₃], which may arise in solution by dissociation from the BPTZ ligand, will not be excited at this wavelength. This transition for free BPTZ occurs at 545 nm; in the mononuclear Nd(III) it has blue-shifted to 523 nm, and in the dinuclear Yb(III) and Er(III) complexes it is further blue shifted by a similar amount to 503 nm. Thus, the effects of the {Ln(tta)₃} units on the position of the absorption maximum of the BPTZ ligand are again approximately additive.

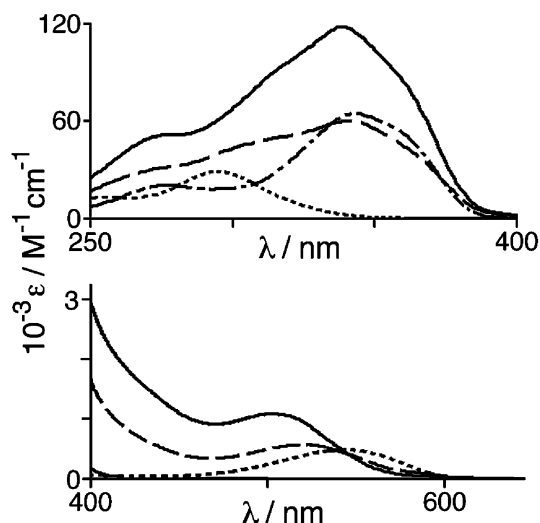**Fig. 4** Electronic spectra in the UV and visible regions of [{Yb-(tta)₃}₂(μ-BPTZ)] (———), [Nd(tta)₃(BPTZ)] (---), BPTZ (···) and [Yb(tta)₃(H₂O)₂] (-·-).

Photophysical properties of the complexes

Excitation of the three complexes at 337 and 520 nm in CH₂Cl₂ and in the solid state resulted in metal-centred luminescence in each case; the lifetimes and calculated quantum yields are summarised in Table 2, and representative spectra are shown in Fig. 5. In every case emission lifetimes are in the microsecond domain and are considerably longer than those of the parent [Ln(tta)₃(H₂O)₂] complexes determined by excitation at 337 nm (included for comparison), because of the replacement of two water ligands—containing four potentially quenching O–H oscillators—by the *N*,*N*-bidentate site of BPTZ in which most of the CH oscillators are more remote from the metal centre. The quantum yield values are estimated from eqn. (3), in which τ_{obs} is the observed emission lifetime and τ_0 is the radiative or 'natural' lifetime, *viz.* 14, 2 and 0.25 ms for Er(III), Yb(III) and Nd(III) respectively.[2a,3]

$$\Phi_{Ln} = \tau_{obs}/\tau_0 \qquad (3)$$
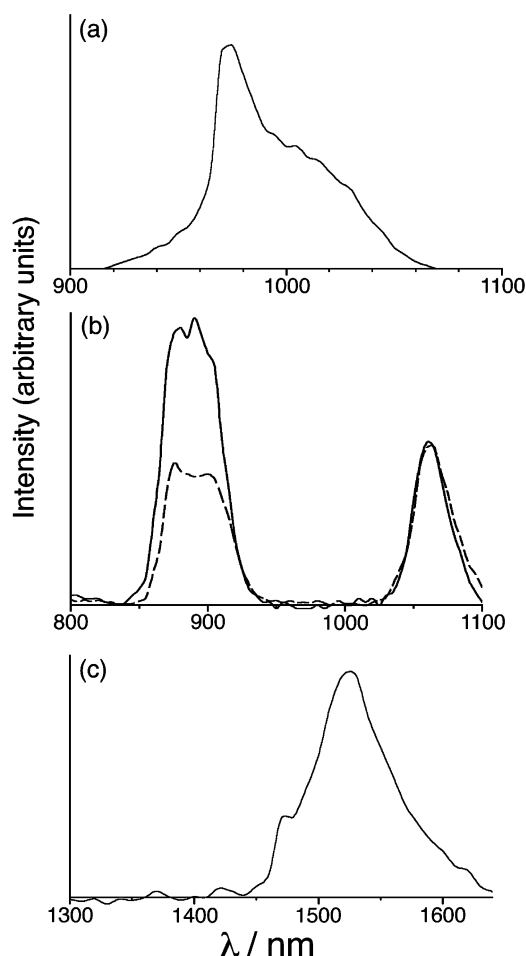
Fig. 5 Uncorrected emission spectra for (a) [{Yb(tta)₃}₂(μ-BPTZ)] in dichloromethane (λ_{exc} = 520 nm); (b) [Nd(tta)₃(BPTZ)] in dichloromethane (solid line) and methanol (dashed line) (λ_{exc} = 337 nm); and (c) [{Er(tta)₃}₂(μ-BPTZ)] in dichloromethane (λ_{exc} = 520 nm).

The lifetime and quantum yield values we obtain are in good agreement with other recently-published results on near-IR luminescent lanthanide complexes,[2–7] indicating that the low-energy electronic transition of the BPTZ ligand does indeed act as a sensitiser for all of these metal ions. We note that time-resolved luminescence measurements from Er(III) complexes are particularly rare.[2,3,5] It is also important to note that the rise-time for the luminescence is within the envelope of the laser pulse (< 5 ns), indicating that energy-transfer from the BPTZ-centred triplet state is fast, as we hoped given that the antenna unit is directly coordinated to the metal centres.

Analysis of the luminescence behaviour of the complexes in solution is complicated by the presence of an equilibrium involving dissociation of the metal fragments in the dinuclear Yb(III) and Er(III) complexes, according to eqns. (4) and (5). These are not exactly the reverse of eqns. (2) and (1) respectively because of the absence of water ligands in this case, but the principle is the same; the fragments denoted '[Ln(tta)₃]' will of course be solvated to some extent by the CH₂Cl₂ solvent.

$$[\{Ln(tta)_3\}_2(\mu\text{-}BPTZ)] = [Ln(tta)_3(BPTZ)] + [Ln(tta)_3] \qquad (4)$$

$$[Ln(tta)_3(BPTZ)] = BPTZ + [Ln(tta)_3] \qquad (5)$$
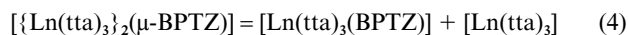
Looking first at the *mono*nuclear complex [Nd(tta)₃(BPTZ)] it is clear that this is well behaved and remains fully associated in CH₂Cl₂ solution under the conditions employed. This is what would be expected at a concentration of *ca.* 10⁻³ M given an association constant of the order of 10⁶ M⁻¹ [by analogy with the La(III) complex, above]. Excitation at 337 nm—which will excite both the intact complex [Nd(tta)₃(BPTZ)] and any free

Table 2 Emission lifetimes (in μs) of luminescence from the complexes in this paper. Quoted lifetimes are ±10%

| Complex | τ/μs | | | ϕ^a |
	CH_2Cl_2, λ_{exc} 337 nm	CH_2Cl_2, λ_{exc} 520 nm	Solid, λ_{exc} 337 nm	
$[Nd(tta)_3(BPTZ)]^b$	0.76	0.78	1.25	3×10^{-3}
$[\{Yb(tta)_3\}_2(\mu\text{-}BPTZ)]^c$	1.0, 13.3^e	14.5	14.1	7×10^{-3}
$[Yb(tta)_3(H_2O)_2]^c$	0.85	—	—	—
$[\{Er(tta)_3\}_2(\mu\text{-}BPTZ)]^d$	0.15, 1.70^e	1.69	2.0	1.2×10^{-4}
$[Er(tta)_3(H_2O)_2]^d$	0.20	—	—	—

^{a} Quantum yield in CH_2Cl_2 solution determined using eqn. (3), from averages of lifetimes measured with 337 nm (longer-lived component) and 520 nm excitation. These values refer to the metal-based process only and do not account for the efficiency of inter-system crossing and energy-transfer processes. ^{b} Luminescence decay measured at 1055 nm. ^{c} Luminescence decay measured at 980 nm. ^{d} Luminescence decay measured at 1530 nm. ^{e} Dual-exponential decay; see main text.

(solvated) $[Nd(tta)_3]$—gave only a single exponential decay ($\tau = 0.76$ μs), characteristic of a single luminescent species being present. Furthermore, it may be seen from Fig. 5(b) that the relative intensities of the two bands in dichloromethane are quite different from those observed in methanol, where the complex dissociates to give $[Nd(tta)_3(MeOH)_n]$. These transitions in Nd(III) complexes are hypersensitive to site symmetry, and the changes observed reflect the presence of different species in different solvents. Confirmation that the complex is intact in dichloromethane (within the limits of sensitivity of the experiment) is provided by excitation at 520 nm which, since it excites only the BPTZ ligand, will result in emission only from intact $[Nd(tta)_3(BPTZ)]$. The appearance of the emission spectrum and the lifetime of the luminescence ($\tau = 0.78$ μs) are both the same, within experimental error, as those obtained using 337 nm excitation. The solid-state emission from $[Nd(tta)_3(BPTZ)]$ however is considerably longer, with $\tau = 1.25$ μs. We ascribe this to the absence of solvent-based quenching in the solid state. Nd(III) is particularly sensitive to quenching by C–H oscillators, because the energy of the lowest luminescent transition ($^4F_{3/2} \longrightarrow {}^4I_{15/2}$; 5400 cm^{-1}) matches well the first overtone of typical C–H vibrations (5900 cm^{-1}).^{6i} In solution the C–H bonds of the CH_2Cl_2 will therefore provide a quenching mechanism which is absent in the solid state, hence the increased luminescence lifetime for the solid material.

The behaviour of the dinuclear complexes $[\{Ln(tta)_3\}_2(\mu\text{-}BPTZ)]$ (Ln = Yb, Er) is different from this. Under 337 nm excitation, the Yb complex shows dual emission, with lifetimes for the two components of 13.3 and 1.0 μs. This is consistent with dissociation of one $[Yb(tta)_3]$ metal fragment according to eqn. (4). Making the approximation that the equilibrium constant for eqn. (4) is $(K_2)^{-1}$, i.e. 1.25×10^{-5} M, at a concentration of 10^{-3} M—typical of the concentrations used for photophysical measurements—we expect about 11% dissociation. On the basis (above) that the mononuclear Nd complex remains fully associated under these conditions, we can rule out the possibility of further dissociation to liberate a second equivalent of $[Yb(tta)_3]$ and free BPTZ [eqn. (5)]. The equilibrium of eqn. (4) will therefore result in three luminescent species in solution; however the good fit of the observed luminescence to a two-component model implies that dinuclear $[\{Yb(tta)_3\}_2(\mu\text{-}BPTZ)]$ (major component) and mononuclear $[Yb(tta)_3(BPTZ)]$ (minor component) have very similar lifetimes, which is reasonable as any structural differences are remote from the metal coordination sphere and will have little effect on quenching. Thus, we assign the longer-lived emission (13.3 μs) to the two BPTZ-containing species $[\{Yb(tta)_3\}_2(\mu\text{-}BPTZ)]$ and $[Yb(tta)_3(BPTZ)]$, and the shorter-lived emission (1.0 μs) to solvated $[Yb(tta)_3]$, for three reasons. Firstly, excitation at 520 nm (which will result in emission only from $[\{Yb(tta)_3\}_2(\mu\text{-}BPTZ)]$ and $[Yb(tta)_3(BPTZ)]$, due to

selective excitation of the BPTZ chromophore) results in luminescence with a single exponential decay, having a lifetime of 14.5 μs, in good agreement with the longer-lived emission arising from 337 nm excitation. Secondly, mononuclear $[Yb(tta)_3(H_2O)_2]$ dissolved in CH_2Cl_2 was found to have an emission lifetime of 850 ns (337 nm excitation); the fact that this is slightly shorter than the 1.0 μs component observed above is because in $[Yb(tta)_3(H_2O)_2]$ the water ligands will be more effective quenchers than weakly-associated CH_2Cl_2 in solvated $[Yb(tta)_3]$ generated by dissociation from the BPTZ complex. Thirdly, the solid-state emission from (intact) $[\{Yb(tta)_3\}_2(\mu\text{-}BPTZ)]$ has a lifetime of $\tau = 14.1$ μs, which agrees well with the values of 14.5 and 13.3 μs obtained in solution. We note that in this case there is no significant difference between the emission lifetimes of $[\{Yb(tta)_3\}_2(\mu\text{-}BPTZ)]$ in the solid state and in solution. Yb(III) is much less sensitive than Nd(III) to quenching by C–H oscillators, so the effect of the CH_2Cl_2 solvent is much less pronounced than it was for $[Nd(tta)_3(BPTZ)]$.

The dinuclear Er(III) complex shows exactly similar behaviour. Using 337 nm excitation, a solution of $[\{Er(tta)_3\}_2(\mu\text{-}BPTZ)]$ in CH_2Cl_2 shows dual-exponential luminescence decay at 1530 nm with τ values of 1.70 and 0.15 μs. The longer component corresponds to intact $[\{Er(tta)_3\}_2(\mu\text{-}BPTZ)]$ and some mononuclear $[Er(tta)_3(BPTZ)]$ arising from the dissociation process of eqn. (4), and the shorter corresponds to solvated (CH_2Cl_2) $[Er(tta)_3]$ which is also produced by this dissociation. In agreement with this, excitation at 520 nm (into the BPTZ absorption) gave a single-exponential decay with $\tau = 1.69$ μs, and excitation of a solution of $[Er(tta)_3(H_2O)_2]$ at 337 nm likewise gave a single-exponential decay, with $\tau = 0.20$ μs. Solid $[\{Er(tta)_3\}_2(\mu\text{-}BPTZ)]$ gave single-exponential luminescence with $\tau = 2.0$ μs, slightly longer than the lifetime in CH_2Cl_2 solution due to the absence of solvent-based quenching.

Conclusions

The BPTZ ligand coordinates to $\{Ln(tta)_3\}$ fragments to give either mononuclear complexes $[Ln(tta)_3(BPTZ)]$ (Ln = Nd or La) or dinuclear complexes $[\{Ln(tta)_3\}_2(\mu\text{-}BPTZ)]$ (Ln = Gd, Yb, Er). Measurements of association constants in CH_2Cl_2 solution for Ln = La and Yb show comparable association constants with a modest diminution of K_2 with respect to K_1 in each case (factors of 2 for La, 3.5 for Yb) which we ascribe to a weak steric interaction between the two $\{Ln(tta)_3\}$ fragments, in agreement with structural data. The fact that only mononuclear complexes were isolated with Ln = La and Nd is assumed to arise from kinetic factors associated with the synthetic method (precipitation from aqueous ethanol). The low-energy absorption of the BPTZ ligand transition in the visible region permits effective sensitisation of near-IR luminescence from the Yb, Nd and Er complexes, with lifetimes on the microsecond timescale, using 520 nm excitation.

Table 3 Crystal, data collection and refinement details for the two structures

Compound	$[\{Yb(tta)_3\}_2(\mu\text{-}BPTZ)]\cdot CH_2Cl_2$	$[\{Gd(tta)_3\}_2(\mu\text{-}BPTZ)]\cdot 2CH_2Cl_2$
Empirical formula	$C_{61}H_{34}Cl_2F_{18}N_6O_{12}S_6Yb_2$	$C_{62}H_{36}Cl_4F_{18}Gd_2N_6O_{12}S_6$
Formula weight	1994.28	2047.62
System, space group	Monoclinic, $P2_1/c$	Monoclinic, $P2_1/n$
$a/\text{Å}$	10.335(7)	10.2615(12)
$b/\text{Å}$	19.431(10)	19.677(3)
$c/\text{Å}$	19.085(11)	19.167(4)
$\beta/°$	105.22(7)	105.384(13)
$V/\text{Å}^3$	3698(4)	3731.3(9)
Z	2	2
Calc. density/Mg m^{-3}	1.791	1.822
Data, restraints, parameters	6516, 24, 492	8581, 0, 498
μ/mm^{-1}	2.861	2.180
$R1$ [$I > 2\sigma(I)$], $wR2^a$	0.0705, 0.1932	0.0495, 0.1177

^{a} The value of $R1$ is based on selected data with $I > 2\sigma(I)$; the value of $wR2$ is based on all data. Data in common: Bruker-AXS SMART diffractometer with Mo-Kα radiation; $T = 173$ K.

Experimental

General details

All reagents, including the ligand BPTZ, were purchased from Aldrich and used as received. UV/Vis spectra were recorded on a Perkin-Elmer Lambda 2 spectrophotometer. Calculations of association constants from UV/Vis spectroscopic titration data were performed with the program NMRTit-HGG (for 1 : 2 BPTZ : lanthanide complexes) kindly provided by Prof. C. A. Hunter of the University of Sheffield.[15]

Syntheses of complexes

All of the metal complexes were prepared in the same general way; the preparation of $[\{Yb(tta)_3\}_2(\mu\text{-}BPTZ)]$ described here is representative. To a solution of Htta (169 mg, 0.76 mmol) and NaOH (30.5 mg, 0.76 mmol) in a mixture of ethanol (10 cm³) and water (3 cm³) was added a solution of YbCl₃·6H₂O (98 mg, 0.25 mmol) in ethanol (5 cm³). The resulting clear yellow solution was stirred for 5 minutes, after which time a solution of BPTZ (30 mg, 0.127 mmol) in ethanol (15 cm³) and added. The resulting clear red–pink solution was stirred for 10 minutes, after which addition of water (25 cm³) resulted in separation of dark-red precipitate, which was filtered, washed with water and hexane, and vacuum dried to give $[\{Yb(tta)_3\}_2(\mu\text{-}BPTZ)]$ as a dark-red solid (149 mg, 61%). Anal. calc. for $Yb_2C_{60}H_{32}O_{12}S_6F_{18}N_6$: C, 37.7; H, 1.7; N, 4.4. Found: C, 37.7; H, 1.5; N, 4.4%.

Exactly the same procedure was used to prepare the complexes listed below.

$[\{Gd(tta)_3\}_2(\mu\text{-}BPTZ)]$. (Dark red). Anal. calc. for $Gd_2C_{60}H_{32}O_{12}S_6F_{18}N_6$: C, 38.4; H, 1.2; N, 4.5. Found: C, 38.6; H, 1.5; N, 4.5%.

$[\{Er(tta)_3\}_2(\mu\text{-}BPTZ)]$. (Dark red). Anal. calc. for $Er_2C_{60}H_{32}O_{12}S_6F_{18}N_6$: C, 38.0; H, 1.7; N, 4.4. Found: C, 37.9; H, 1.5; N, 4.5%.

$[La(tta)_3(BPTZ)]$. (Bright pink). Anal. calc. for $LaC_{36}H_{20}O_6S_3F_9N_6$: C, 41.6; H, 1.9; N, 8.1. Found: C, 41.5; H, 1.7; N, 7.9%.

$[Nd(tta)_3(BPTZ)]$. (Bright pink). Anal. calc. for $NdC_{36}H_{20}O_6S_3F_9N_6$: C, 41.4; H, 1.9; N, 8.1. Found: C, 41.1; H, 1.7; N, 8.1%.

Crystallography

For each complex a suitable crystal was coated with hydrocarbon oil and attached to the tip of a glass fibre, which was then transferred to a Bruker-AXS SMART diffractometer under a stream of cold N₂ at 173 K. Details of the crystal parameters, data collection and refinement for each of the structures are collected in Table 3. After data collection, in each case an empirical absorption correction (SADABS) was applied,[16] and the structures were then solved by conventional direct methods and refined on all F^2 data using the SHELX suite of programs.[17] In all cases, non-hydrogen atoms were refined with anisotropic thermal parameters; hydrogen atoms were included in calculated positions and refined with isotropic thermal parameters which were *ca.* 1.2 × (aromatic CH) or 1.5 × (Me) the equivalent isotropic thermal parameters of their parent carbon atoms.

Both complexes have imposed inversion symmetry, with one metal ion and its associated three tta ligands and one half of the bridging ligand being unique. Each asymmetric unit also contains a molecule of CH₂Cl₂, which refined with site occupancy of 0.5 for $[\{Yb(tta)_3\}_2(\mu\text{-}BPTZ)]\cdot CH_2Cl_2$ and 1.0 for $[\{Gd(tta)_3\}_2(\mu\text{-}BPTZ)]\cdot 2CH_2Cl_2$. In the structure of $[\{Gd(tta)_3\}_2(\mu\text{-}BPTZ)]\cdot 2CH_2Cl_2$ two of the three unique thiophene rings are disordered by 180° rotation about the bond connecting it to the diketonate unit, such that the S atom and the C³ atom are mutually disordered; the two components could be refined satisfactorily with the superimposed fractional S and C atoms being constrained to have identical positional and thermal parameters [S(16)/C(19), 0.81 : 0.19 site occupancies; S(36)/C(39), 0.63 : 0.37 site occupancies]. H atoms were not included in the refinement for these disordered C atoms.

CCDC reference numbers 200935 and 200936.

See http://www.rsc.org/suppdata/dt/b3/b300294b/ for crystallographic data in CIF or other electronic format.

Luminescence studies

Solution state measurements. The sample was excited using a pulsed nitrogen laser (PTI-3301, 337 nm) or a nitrogen pumped dye laser (PTI-330, 520 nm), operating at 10 Hz. Light emitted right angles to the excitation beam was focused onto the slits of a monochromator (PTI120), which was used to select the appropriate wavelength. The growth and decay of the luminescence at selected wavelengths was detected using a germanium photodiode (Edinburgh Instruments, EI–P) and recorded using a digital oscilloscope (Tektronix TDS220) before being transferred to a PC for analysis. Time-resolved emission spectra were obtained by measuring the growth and decay of the luminescence at each of a series of wavelengths. Luminescence lifetimes were obtained by iterative reconvolution of the detector response (obtained by using a scatterer) with exponential components for growth and decay of the metal centred luminescence, using a spreadsheet running in Microsoft Excel. The details of this approach have been discussed elsewhere.[7d,e,h] Unless otherwise stated, fitting to a double exponential decay

yielded no improvement in fit as judged by minimisation of residual squared and reduced chi squared.

Luminescence from solid samples. The sample was excited using a pulsed nitrogen laser (PTI-3301, 337 nm) or a nitrogen pumped dye laser (PTI-330, 520 nm), operating at 10 Hz and incident on a flat sample surface set at 30° to the incident beam. Light emitted right angles to the excitation beam was focused onto the slits of a monochromator (PTI120), which was used to select the appropriate wavelength. The growth and decay of the luminescence at selected wavelengths was detected using a germanium photodiode (Edinburgh Instruments, EI–P) and recorded using a digital oscilloscope (Tektronix TDS220) before being transferred to a PC for analysis. Data analysis was carried out using the techniques described above.

Acknowledgements

References

1 M. P. Bailey, B. F. Rocks and C. Riley, *Analyst (London)*, 1984, **109**, 1449; J. Coates, P. G. Sammes, G. Yahioglu, R. M. West and A. J. Garman, *J. Chem. Soc., Chem. Commun.*, 1994, 2311; R. R. De Haas, N. P. Verwoerd, M. P. van der Corput, R. P. van Gijlswijk, H. Siitari and H. J. Tanke, *J. Histochem. Cytochem.*, 1996, **44**, 1091; M. Montalti, L. Prodi, N. Zaccheroni, L. Charbonniere, L. Douce and R. Ziessel, *J. Am. Chem. Soc.*, 2001, **123**, 12694; A. Mayer and S. Neuenhofer, *Angew. Chem., Int. Ed. Engl.*, 1994, **33**, 1044; A. Beeby, I. M. Clarkson, S. Faulkner, S. W. Botchway, D. Parker, A. W. Parker and J. A. G. Williams, *J. Photochem. Photobiol. B: Biol.*, 2000, **57**, 83; D. Parker, R. S. Dickins, H. Puschmann, C. Crossland and J. A. K. Howard, *Chem. Rev.*, 2002, **102**, 1977.
2 (*a*) S. I. Klink, L. Grave, D. N. Reinhoudt, F. C. J. M. van Veggel, M. H. V. Werts, F. A. J. Geurts and J. W. Hofstraat, *J. Phys. Chem. A*, 2000, **104**, 5457; (*b*) S. I. Klink, G. A. Hebbink, L. Grave, F. C. J. M. van Veggel, D. N. Reinhoudt, L. H. Slooff, A. Polman and J. W. Hofstraat, *J. Appl. Phys.*, 1999, **86**, 1181; (*c*) S. I. Klink, G. A. Hebbink, L. Grave, F. G. A. Peters, F. C. J. M. van Veggel, D. N. Reinhoudt and J. W. Hofstraat, *Eur. J. Org. Chem.*, 2000, 1923.
3 G. A. Hebbink, D. N. Reinhoudt and F. C. J. M. van Veggel, *Eur. J. Org. Chem.*, 2001, 4101.
4 G. A. Hebbink, S. I. Klink, L. Grave, P. G. B. Oude Alink and F. C. J. M. van Veggel, *Chem. Phys. Chem.*, 2002, **3**, 1014.
5 (*a*) M. H. V. Werts, J. W. Verhoeven and J. W. Hofstraat, *J. Chem. Soc., Perkin Trans. 2*, 2000, 433; (*b*) M. P. Oude Wolbers, F. C. J. M. van Veggel, F. G. A. Peters, E. S. E. van Beelen, J. W. Hofstraat, F. A. J. Geurts and D. N. Reinhoudt, *Chem. Eur. J.*, 1998, **4**, 772; (*c*) M. H. V. Werts, J. W. Hofstraat, F. A. J. Geurts and J. W. Verhoeven, *Chem. Phys. Lett.*, 1997, **276**, 196; (*d*) J. W. Hofstraat, M. P. Oude Wolbers, F. C. J. M. van Veggel, D. Reinhoudt, M. H. V. Werts and J. W. Verhoeven, *J. Fluoresc.*, 1998, **8**, 301.
6 (*a*) M. Asano-Someda and Y. Kaizu, *J. Photochem. Photobiol. A*, 2001, **139**, 161; (*b*) A. I. Voloshin, N. M. Shavaleev and V. P. Kazakov, *J. Lumin.*, 2001, **93**, 115; (*c*) Y. V. Korovin, S. B. Meshkova and N. S. Poluektov, *J. Anal. Chem. USSR*, 1984, **39**, 234; (*d*) Y. Hasegawa, K. Murakoshi, Y. Wada, S. Yanagida, J. H. Kim, N. Nakashima and T. Yamanaka, *Chem. Phys. Lett.*, 1996, **248**, 8; (*e*) W. D. Horrocks, J. P. Bolender, W. D. Smith and R. M. Supkowski, *J. Am. Chem. Soc.*, 1997, **119**, 5972; (*f*) H. Hasegawa, T. Ohkubo, K. Sogabe, Y. Kawamura, Y. Wada, N. Nakashima and S. Yanagida, *Angew. Chem., Int. Ed.*, 2000, **39**, 357; (*g*) M. Iwamuro, Y. Wada, T. Kitamura, N. Nakashima and S. Yanagida, *Phys. Chem. Chem. Phys.*, 2000, **2**, 2291; (*h*) Y. Wada, T. Okubo, M. Ryo, T. Nakazawa, Y. Hasegawa and S. Yanagida, *J. Am. Chem. Soc.*, 2000, **122**, 8583; (*i*) S. Yanagida, Y. Hasegawa, K. Murakoshi, Y. Wada, N. Nakashima and T. Yamanaka, *Coord. Chem. Rev.*, 1998, **171**, 461.
7 (*a*) A. Beeby, R. S. Dickins, S. Faulkner, D. Parker and J. A. G. Williams, *Chem. Commun.*, 1997, 1401; (*b*) J. Hall, R. J. Haner, S. Aime, M. Botta, S. Faulkner, D. Parker and J. A. G. Williams, *New J. Chem.*, 1998, **22**, 627; (*c*) S. Faulkner, A. Beeby, R. S. Dickins, D. Parker and J. A. G. Williams, *J. Fluoresc.*, 1999, **9**, 45; (*d*) A. Beeby and S. Faulkner, *Chem. Phys. Lett.*, 1997, **266**, 116; (*e*) A. Beeby, S. Faulkner, D. Parker and J. A. G. Williams, *J. Chem. Soc., Perkin Trans. 2*, 2001, 1268; (*f*) A. Beeby, I. M. Clarkson, R. S. Dickins, S. Faulkner, D. Parker, L. Royle, A. S. de Sousa, J. A. G. Williams and M. Woods, *J. Chem. Soc., Perkin Trans. 2*, 1999, 493; (*g*) A. Beeby, B. P. Burton-Pye, S. Faulkner, J. C. Jeffery, J. A. McCleverty, G. R. Motson and M. D. Ward, *J. Chem. Soc., Dalton Trans.*, 2002, 1923; (*h*) A. Beeby, S. Faulkner and J. A. G. Williams, *J. Chem. Soc., Dalton Trans.*, 2002, 1918; (*i*) C. Reinhard and H. U. Güdel, *Inorg. Chem.*, 2002, **41**, 1048.
8 M. J. Weber, *Lanthanide and Actinide Chemistry and Spectroscopy*, American Chemical Society, Washington DC, 1980, p. 275.
9 (*a*) R. J. Mears and S. R. Baker, *Opt. Quantum Electron.*, 1992, **24**, 517; (*b*) E. Desurvire, *Phys. Today*, 1994, **97**, 20; (*c*) E. Desurvire, *Erbium-doped amplifiers. Principles and Applications*, John Wiley & Sons, New York, 1994; (*d*) Y. Oshishi, T. Kanamori, Y. Kitagawa, S. Takashashi, E. Snitzer and G. H. Sigel, Jr., *Opt. Lett.*, 1991, **16**, 1747.
10 N. Sabbatini, M. Guardigli and J.-M. Lehn, *Coord. Chem. Rev.*, 1993, **123**, 201.
11 S. Sato and M. Wada, *Bull. Chem. Soc. Jpn.*, 1970, **43**, 1955.
12 (*a*) K. Iftikhar, M. Sayeed and N. Ahmad, *Inorg. Chem.*, 1982, **21**, 80; (*b*) W. H. Watson, R. J. Williams and N. R. Stemple, *J. Inorg. Nucl. Chem.*, 1982, **34**, 501; (*c*) S. Yajima and Y. Hasegawa, *Bull. Chem. Soc. Jpn.*, 1998, **71**, 2825.
13 (*a*) N. M. Shavaleev, Z. R. Bell and M. D. Ward, *J. Chem. Soc., Dalton Trans.*, 2002, 3925; (*b*) N. M. Shavaleev, Z. R. Bell, G. Accorsi, and M. D. Ward, *Inorg. Chim. Acta*, submitted.
14 The coordination chemistry of BPTZ has been reviewed recently: W. Kaim, *Coord. Chem. Rev.*, 2002, **230**, 126.
15 A. P. Bisson, C. A. Hunter, J. C. Morales and K. Young, *Chem. Eur. J.*, 1998, **4**, 845.
16 G. M. Sheldrick, SADABS, A program for absorption correction with the Siemens SMART area-detector system, University of Göttingen, 1996.
17 G. M. Sheldrick, SHELXS-97 and SHELXL-97 programs for crystal structure solution and refinement, University of Göttingen, 1997.